EPJ Web of Conferences 70, 00008 (2014)
DOI: 10.1051/epjconf/20147000008

Recent Results from Experiment D0

V. Šimák

[1] *FZU ACR and FJFI CTU Prague, for D0 Experiment*

Abstract. Brief summary of resent experimental results from experiment D0 at TEVATRON in FNAL.

1 Introduction

After 28 years (1983 - 2011) of TEVATRON work in FNAL, particle physics reach high level of understanding of elementary interactions in center of mass energy up to 2 TeV. Two big particle detector, CDF and D0 could analyze all interactions detected with complex of subdetectors in full 4π cover and with magnetic spectrometry for all charged particles.

Briefs summary of some of results achieved at TEVATRON:
1985 - First observation of proton-antiproton collisions by CDF at 1.8 TeV (June 8).
1992 - D0 observes first proton-antiproton collision with cms energy 1.8 TeV.
1995 - Experiment CDF ad D0 announce discovery of top quark (March 3th).
1996 - Observation of antihydrogen atoms.
1996 - Observation of exotic charm meson.
1998 - Discovery of B_c meson.
1999 - Fixed target experiment KTeV observes direct CP violation in the decay of neutral Kaons.
2000 - The DONuT experiment reports first evidence for the direct observation of the τ neutrino.
2004 - Run II, which started in 2001, achieves a peak luminosity 10^{32} cm^2 sec^{-1}.
2006 - Discovery of Bs matter-antimatter oscillations 3 trillion times per second.
2007 - Discovery of cascade b-baryon.
2009 - Discovery of single top quark production.
2010 - Tevatron achieves a peak luminosity $4x10^{32}$ cm^2 sec^{-1}
2011 - Tevatron produces final pron-antiproton collisions (sept 30)

Experiments D0 and CDF have collected about 10 fb^{-1} of data each.

The result from both experiment enriched knowledge in particle physics and
fulfilled some open questions in Standard Model.
The analysis of data will still continue for few next years.

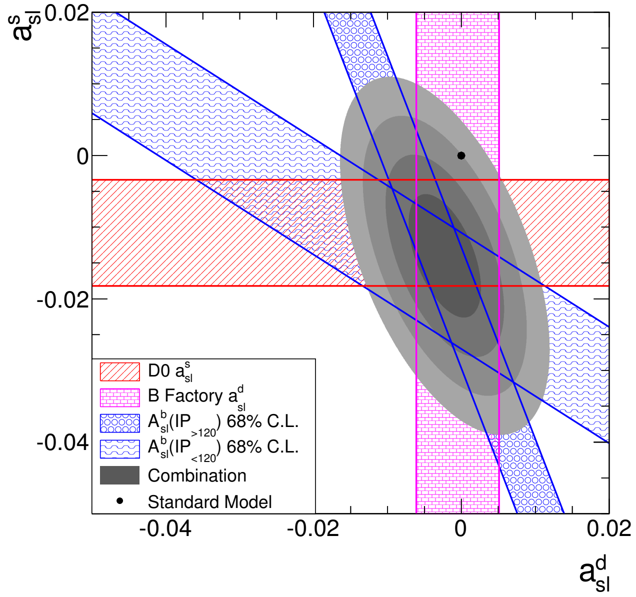

Figure 1. Combination of D0 and B factory average for a^d_{sl} and a^s_{sl}.

Following pictures present resent results from experiment D0 divided according the subjects: B-physics, Electroweek physics, Quntum Chromodynamics, Top quark physics, Higgs boson and New Phenomena. Most of the results are obtained with statistics of events corresponding to $10.4 fb^{-1}$.

2 B-physics

Several results in spectroscopy of hadrons from is coming from study of physics of b quark, which could be directly identified in 60% of events. We present a measurement of the semileptonic mixing asymmetry $a = (\Gamma(\bar{A}) - \Gamma(A))/(\Gamma(\bar{A}) + \Gamma(A))$ for B^0 mesons, a^d_{sl}. Using two independent decay channels: $B^0 \to \mu + D + X$, $D \to K^+\pi^-\pi^-$ and $B^0 \to \mu + D^* + X$, $B^0 \to \mu + D^* + X$ with $D^* \to \bar{D}^0 + \pi^-$, $\bar{D}^0 \to K^+\pi^-$ (and charge conjugate processes), we have determined the semileptonic mixing asymmetry for B^0 mesons, a^d_{sl}. We extract the charge asymmetries in these two channels as a function of the visible proper decay length (VPDL) of the B0 meson, correct for detector-related asymmetries using data-driven methods, and account for dilution from charge-symmetric processes using Monte Carlo simulation. The final measurement combines four signal VPDL regions for each channel, yielding:

$a^d_{sl} = 0.68 \pm 0.45$ (stat.) ± 0.14 (syst.)

Combination of measurements of a^d_{sl} (D0 and existing world-average from B factories), a^s_{sl}, and the two impact-parameter-binned constraints from the same-charge dimuon asymmetry A^b_{sl}. The bands represent the ± 1 standard deviation uncertainties on each measurement. The ellipses represent the 1, 2, 3, and 4 standard deviation twodimensional confidence level regions of the combination [1] in Fig.2.

We have measure the time-integrated flavor-specific semileptonic charge asymmetry in the decays of B^0_s mesons that have undergone flavor mixing, a^s_{ls}, using $B^0_s(\bar{B}^0_s) \to D^{\pm}_s + \mu^+ + X$ decays, with $D^{\pm}_s \to \phi\pi^{\pm}$ and $\phi \to K^+K^-$. of proton-antiproton collisions.

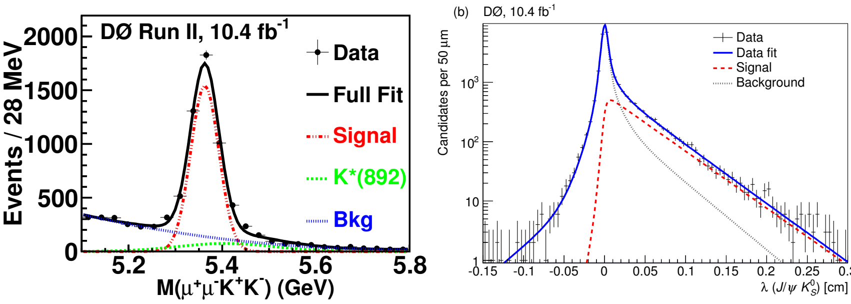

Figure 2. Invariant mass distribution of B_s^0 candidates with $ct > 200\mu m$ for events in the mass range $1.01 < M(K^+K^-) < 1.03GeV$. A fit to a sum of a Gaussian $B_s^0 \to J/\psi\phi$ signal (dashed-dotted) a quadratic combinatorial background (dotted), and the reflection of the decay $B^0 \to J/\psi K^*(892)$ (dashed), is used to extract the B_s^0 yield (left). Proper decay length distributions for $B^0 \to J/K^0$ candidates, with fit results superimposed (right).

A fit to the difference between the time-integrated D_s^- and D_s^+ mass distributions of the B_s^0 and $\bar{B}^{0_s}$ candidates yields the flavor-specific asymmetry

$a_{ls}^s = -1.08 \pm 0.72(stat) \pm 0.17(syst)$

which is the most precise measurement and in agreement with the standard model prediction. We have investigated the decay $B_s^0 \to J/\psi \to K^+K^-$ for invariant masses of the K^+K^- pair in the range $1.35 < M(K^+K^-) < 2GeV$ Fig.2.

From the study of the invariant mass and spin of the K^+K^- system, we find evidence for the two-body decay and measure the relative branching fraction of the decays to be [2] $R_{f_2'/\phi} = 0.22 \pm 0.05$ (stat) $\pm$ 0.04 (syst). We measure the Λ_b^0 lifetime in the fully reconstructed decay $\Lambda_b^0 \to J/\psi\Lambda^0$ [3] Fig. 2.

The lifetime of the topologically similar decay channel $B^0 \to J/\psi K_S^0$ is also measured [4]. We obtain

$\tau(\Lambda_b^0) = 1.303 \pm 0.075(stat.) \pm 0.035(syst.)ps$

and $\tau(B^0) = 1.508 \pm 0.025(stat.) \pm 0.043(syst.)ps$.

Using these measurements, we determine the lifetime ratio of

$\tau(\Lambda_b^0)/\tau(B^0) = 0.864 \pm 0.052(stat.) \pm 0.033(syst.)$.

We present a measurement of the relative branching fraction, $R_{f_0/\phi}$, of B_s^0 to $J/\psi f_0(980)$, with $f_0(980) \to \pi^+\pi^-$, to the process $B_s^0 \to J/\psi\phi$, with $\phi \to K^+K^-$ Fig. 2. The $J/\psi f_0(980)$ final state corresponds to a CP-odd eigenstate of B_s^0 that could be of interest in future studies of CP violation.

With $8fb^{-1}$ of data recorded with the D0 detector we find

$R_{f_0/\phi} = 0.275 \pm 0.041(stat) \pm 0.061(syst)$.

Using data corresponding to an integrated luminosity of $1.3fb^{-1}$, we observe a narrow mass state decaying into $\upsilon(1S) + \gamma$, where the $\upsilon(1S)$ meson is detected by its decay into a pair of oppositely charged muons, and the photon is identified through its conversion into an electron-positron pair. The significance of this observation is 5.6 standard deviations. The mass of the state is centered at $10.551 \pm 0.014(stat.) \pm 0.017(syst.)GeV/c^2$, which is consistent with that of the state recently observed by the ATLAS Collaboration Fig.3 [5].

3 Electroweek Interactions

Mass measurement of W mass combined from experiments CDF and D0 are in Fig. 4 [6].

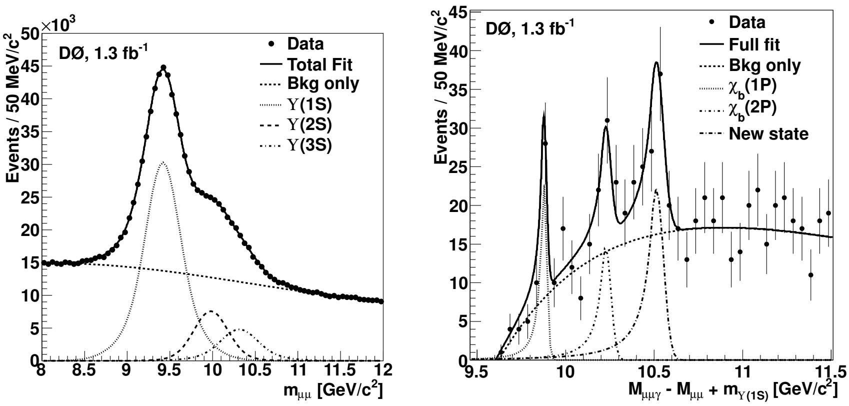

Figure 3. Dimuon invariant mass spectrum for opposite-charge pairs passing the muon selection criteria. The solid curve is a fit to the data assuming three υ resonances and a combinatorial background. The relative contributions from the $\upsilon(1S)$, $\upsilon(2S)$, and $\upsilon(3S)$ (left). The distribution of $M_{\mu\mu\gamma}$ - $M\mu\mu$ + $m_{\upsilon(1S)}$ fit with three signal functions and the mixed event background (right).

We present a measurement of the W boson mass using data corresponding to $4.3fb^{-1}$ of integrated luminosity collected with the D0 detector during Run II at the Fermilab Tevatron $p\bar{p}$ collider. With a sample of 1,677,394 decay $W \to e$ or μ candidate events, we measure $M_W = 80.367 \pm 0.026GeV$. This result is combined with an earlier D0 result determined using an independent Run II data sample, corresponding to $1fb^{-1}$ of integrated luminosity, to yield $M_W = 80.375 \pm 0.023GeV$ [7].

We study the processes $p\bar{p} \to WZ \to \ell\nu, \ell^+\ell^-$ and $p\bar{p} \to ZZ \to \ell^+\ell^-\nu\bar{\nu}$ where $\ell = e$ or μ. Using 8.6 fb^{-1} of integrated luminosity. We measure the WZ production cross section to be $4.50^{+0.63}_{-0.66}$ pb which is consistent with, but slightly above a prediction of the standard model. The ZZ cross section is measured to be 1.64 ± 0.46 pb, in agreement with a prediction of the standard model. Combination with an earlier analysis of the $ZZ \to \ell^+\ell^-\ell^+\ell^-$ channel yields a ZZ cross section of $1.44^{+0.35}_{-0.34}$ pb [9].

We study WW and WZ production with $l\nu qq$ ($l = e, \mu$) final states using data corresponding to$4.3fb^{-1}$ of integrated luminosity. Assuming the ratio between the production cross sections $\sigma(WW)$ and $\sigma(WZ)$ as predicted by the standard model, we measure the total WV (V=W,Z) cross section to be $\sigma(WV) = 19.6^{+3.2}_{-3.0}$ pb, and reject the background-only hypothesis at a level of 7.9 standard deviations. We also use b-jet discrimination to separate the WZ component from the dominant WW component. Simultaneously fitting WW and WZ contributions, we measure $\sigma(WW) = 15.9^{+3.7}_{-3.2}$ pb and $\sigma(WZ) = 3.3^{+4.1}_{-3.3}$ pb, which is consistent with the standard model predictions [8].

We present a measurement of $p\bar{p} \to Z\gamma \to ll + \gamma, l = e, \mu$ production with a data sample corresponding to an integrated luminosity of $6.2fb^{-1}$. The results of the electron and muon channels are combined, and we measure the total production cross section and the differential cross section $d\sigma/dp_T^\gamma$, where p_T^γ is the momentum of the photon in the plane transverse to the beamline Fig. 5. The results obtained are consistent with the standard model predictions from next-to-leading order calculations. We use the transverse momentum spectrum of the photon to place limits on anomalous $ZZ\gamma$ and $Z\gamma\gamma$ couplings [9]. We measure the cross section and the difference in rapidities between photons and charged leptons for inclusive $W \to l\nu + \gamma$ production in $e\gamma$ and $\mu\gamma$ final states. Using data corresponding to an integrated luminosity of $4.2fb^{-1}$, the cross section multiplied by the branching fraction for the process $p\bar{p} \to W\gamma + X \to l\nu\gamma + X$, measured to be 15.8 ± 0.8 (stat.) $\pm 1.2(syst.)$ pb,

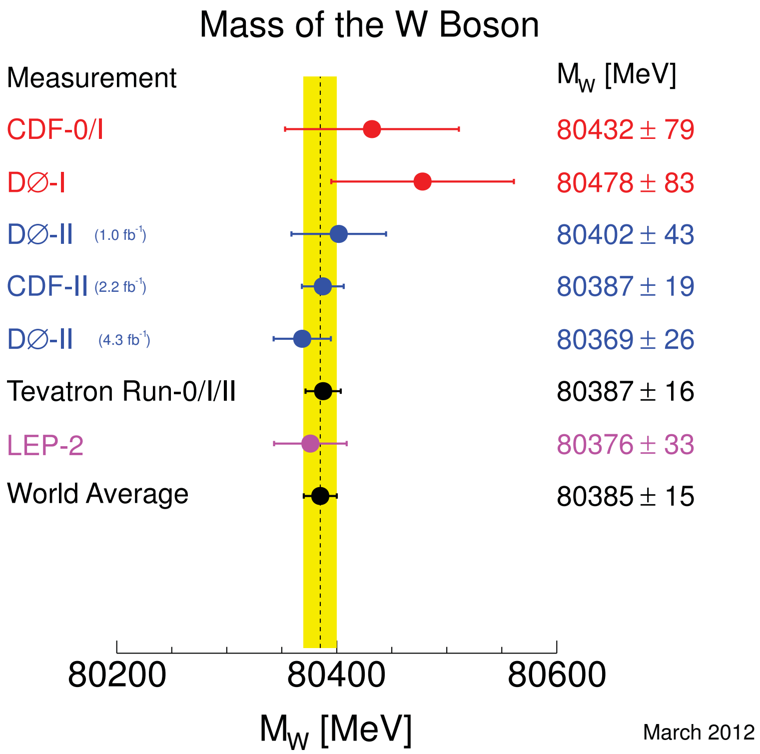

Figure 4. Summary of measurement of W mass as March 2012

and the distribution of the charge-signed photon-lepton rapidity difference are found to be in agreement with the standard model. These results provide the most stringent limits on anomalous $WW\gamma$ couplings for data from hadron colliders: $-0.4 < \Delta\kappa_\gamma < 0.4$ and $-0.08 < \lambda_\gamma < 0.07$ at the 95% C.L.

4 QCD Interactions

We present a measurement of the average value of a new observable at hadron colliders that is sensitive to QCD dynamics and to the strong coupling constant, while being only weakly sensitive to parton

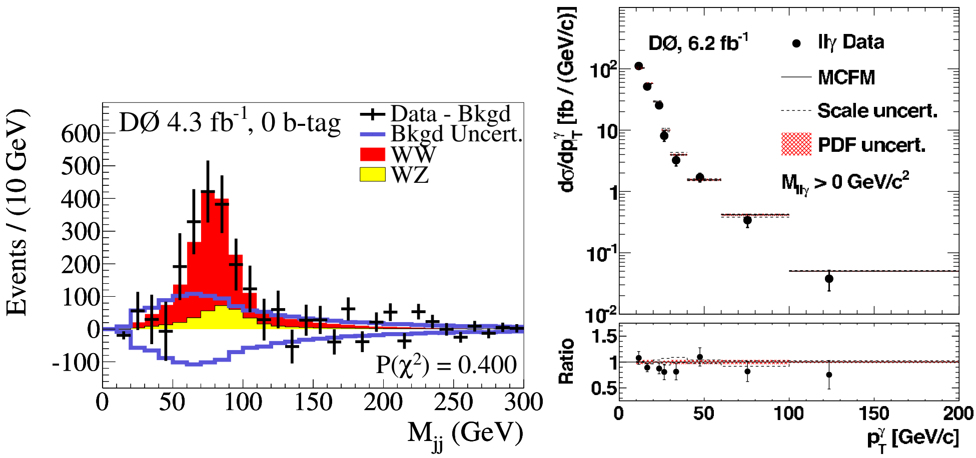

Figure 5. A comparison of the measured WW and WZ signals (filled histograms) to background-subtracted data (points) in the dijet mass distribution (summed over electron and muon channels) for 0, 1, and 2-tag sub-channels after the combined fit to data using the dijet mass distribution [9] (left). Unfolded $d\sigma/dp^{\gamma}_{pT}$ distribution with no $M_{ll\gamma}$ requirement for combined electron and muon data compared to the NLO prediction (right).

distribution functions. The observable measures the angular correlations of jets and is defined as the number of neighboring jets above a given transverse momentum threshold which accompany a given jet within a given distance ΔR in the plane of rapidity and azimuthal angle. The ensemble average over all jets in an inclusive jet sample is measured and the results are presented as a function of transverse momentum of the inclusive jets, in different regions of !R and for different transverse momentum requirements for the neighboring jets. The measurement is based on a data set corresponding to an integrated luminosity of $0.7 fb^{-1}$. The results are well described by a perturbative QCD calculation in next-to-leading order in the strong coupling constant, corrected for non-perturbative effects. From these results, we extract the strong coupling and test the QCD predictions for its running over a range of momentum transfers of 50 to 400 GeV [10] Fig. 6.

We present measurements of the differential cross section $d\sigma/dp_{T\gamma}$ for the inclusive production of a photon in association with a b-quark jet for photons with rapidities $|y_\gamma| < 1.0$ and $30 < p_{T\gamma} < 300 GeV$, as well as for photons with $1.5 < |y_\gamma| < 2.5$ and $30 < p_{T_\gamma} < 200 GeV$, where $p_{T\gamma}$ is the photon transverse momentum Fig. 8. The b-quark jets are required to have $pT > 15 GeV$ and rapidity $|y_{jet}| < 1.5$. The results are based on data corresponding to an integrated luminosity of $8.7 fb^{-1}$. The measured cross sections are compared with next-to-leading order perturbative QCD calculations using different sets of parton distribution functions as well as to predictions based on the kT-factorization QCD approach, and those from the Sherpa and Pythia Monte Carlo event generators [11].

In special runs of D0 experiment with Proton Forward Detector we have meured elastic scattering of $p\bar{p}$ at $\sqrt(s) = 1.960 TeV$. Comparison with other experiments is displayed in Fig. refQCD-3ab [12]. We investigate the decay $B^0_s \to J/\psi K^+K^-$ for invariant masses of the K^+K^- pair in the range $1.35 < M(K^+K^-) < 2$ GeV. The data sample corresponds to an integrated luminosity of 10.4 fb^{-1} of $p\bar{p}$ collisions at $\sqrt{s} = 1.96$ TeV. From the study of the invariant mass and spin of the K^+K^- system, we find evidence for the two-body decay and measure the relative branching fraction of the decays to be $R_{f'_2/\phi} = 0.22 \pm 0.05\,(\text{stat}) \pm 0.04\,(\text{syst})$.

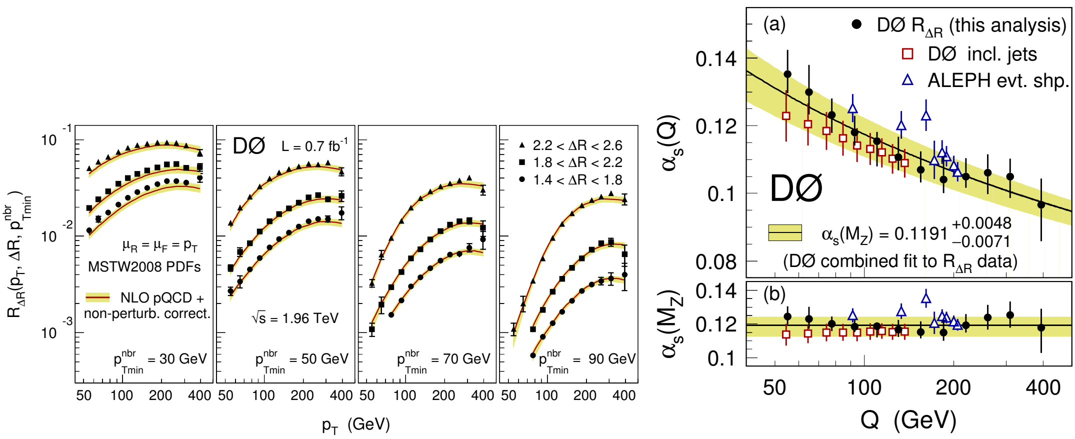

Figure 6. The measurement of $R_{\Delta R}$ as a function of inclusive jet p_T for three different intervals in ΔR and for four different requirements of p_{Tmin}^{nbr}. The inner uncertainty bars indicate the statistical uncertainties, and the total uncertainty bars display the quadratic sum of the statistical and systematic uncertainties. The theory predictions are shown with their uncertainties (left). The strong coupling α_s at large momentum transfers, Q, presented as $\alpha_s(Q)$ (a) and evolved to M_Z using the RGE (b). The uncertainty bars indicate the total uncertainty, including the experimental and theoretical contributions. The new α_s results from $R_{\Delta R}$ are compared to previous results obtained from inclusive jet cross section data. The α_s (MZ) result from the combined fit to all selected data points and the corresponding RGE prediction are also shown (right).

5 TOP quark Physics

The top quark is the heaviest known elementary particle, with a mass about 40 times larger than the mass of its isospin partner, the bottom quark. It decays almost 100%. of the time to a W boson and a b quark. The summary of cross section production of $t\bar{t}$ is presented in Fig. 9, with final combination: $\sigma_{t\bar{t}} = 7.65 \pm 0.42 pb$.

We present a measurement of the top quark mass (m_t) in $p\bar{p}$ collisions at $\sqrt{s}$ = 1.96 TeV using $t\bar{t}$ events with two leptons (ee, $e\mu$, or $\mu\mu$) and accompanying jets in $4.3 fb^{-1}$ of data collected. We analyze the kinematically underconstrained dilepton events by integrating over their neutrino rapidity distributions. We reduce the dominant systematic uncertainties from the calibration of jet energy using a correction obtained from $t\bar{t}$ events with a final state of a single lepton plus jets. We also correct jets in simulated events to replicate the quark flavor dependence of the jet response in data. We measure m_t = 173.7 ± 2.8 (stat) ± 1.5 (syst) GeV and combining with our analysis in 1 fb^{-1} of preceding data we measure m_t = 174.0 ± 2.4 (stat) ± 1.4 (syst) GeV. Taking into account statistical and systematic correlations, a combination with the D0 matrix element result from both data sets yields m_t = 173.9 ± 1.9 (stat) ± 1.6 (syst) GeV [13].

We measure lepton angular distributions in $t\bar{t} \to W^+b, W^-\bar{b} \to l^+\nu\bar{b}l^-$. Using data corresponding to an integrated luminosity of $5.4 fb^{-1}$, we find that the angular distributions of l^- relative to anti-protons and l^+ relative to protons are in agreement with each other. Combining the two distributions and correcting for detector acceptance we obtain the forward-backward asymmetry

$A^l_{FB} = (5.8 \pm 5.1(stat) \pm 1.3(syst))$

compared to the standard model prediction of $A^l_{FB}(predicted) = (4.7 \pm 0.1)$. This result is further combined with the measurement based on the analysis of the l+jets final state to obtain

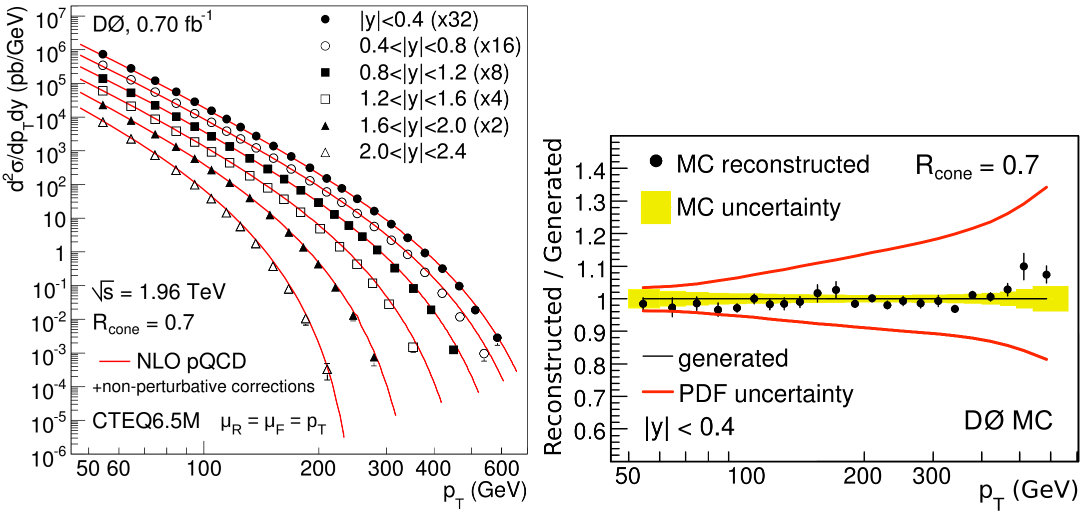

Figure 7. Inclusive jet cross section measurements as a function of jet p_T in six $|y|$ bins. The data points are multiplied by 2, 4, 8, 16, and 32 for the bins $1.6 < |y| < 2.0, 1.2 < |y| < 1.6, 0.8 < |y| < 1.2, 0.4 < |y| < 0.8$, and $|y| < 0.4$, respectively (left). MC closure test of the method used to extract the inclusive jet p_T cross section for the jet $|y| < 0.4$ bin. The full analysis was repeated treating MC events as data and comparing the result to the input cross section. Good agreement is found within the statistical uncertainties of fits to jet energy scale and resolution, and unfolding present in MC (shaded band), which are much smaller than the systematic uncertainties in data(right).

$A^l_{FB} = (11.8 \pm 3.2)$ [14].

We present measurements of the tWb coupling form factors using information from electroweak single top quark production and from the helicity of W bosons from top quark decays in $t\bar{t}$ events Fig. 10 [15]. We set upper limits on anomalous tWb coupling.

Combining measurements that simultaneously determine the fractions of W bosons with longitudinal (f^0) and right-handed (f^+) helicities, we find

$f^0 = 0.722 \pm 0.081[\pm 0.062(stat.) \pm 0.052(syst.)]$ and

$f^+ = -0.033 \pm 0.046[\pm 0.034(stat.) \pm 0.031(syst.)]$.

Combining measurements where one of the helicity fractions is fixed to the value expected in the standard model, we find

$f^0 = 0.682 \pm 0.057[\pm 0.035(stat.) \pm 0.046(syst.)]$ and

$f+ = -0.015 \pm 0.035[\pm 0.018(stat.) \pm 0.030(syst.)]$ [16].

The results are consistent with standard model expectations.

The $t\bar{t}$ spin correlation strength C is defined by

$d^2\sigma_{t\bar{t}}/dcos\Theta_1 dcos\Theta_2 = \sigma_(t\bar{t})\ (1 - Ccos(\Theta_1)cos(\Theta_2))/4$,

where Θ_1, Θ_2 are the angles between the spin-quantization axis and the direction of flight of the down-type fermion from the W boson decay in the respective parent t or $\bar{t}$ rest frame. The fractional difference in the number of events where the top and antitop quark spins are aligned and those where the top quark spins have opposite alignment A is defined as $C = A|\alpha_1\alpha_2|$ where α_i is the spin analyzing power of the final state parton under consideration. In NLO QCD $\alpha_{l^+} = 1$ for the charged lepton in $t \to l{+}\nu_l b$ decays and $\alpha_{\bar{d}} = 0.97$ for the anti-down quark in $t \to \bar{d}ub$ decays. To distinguish

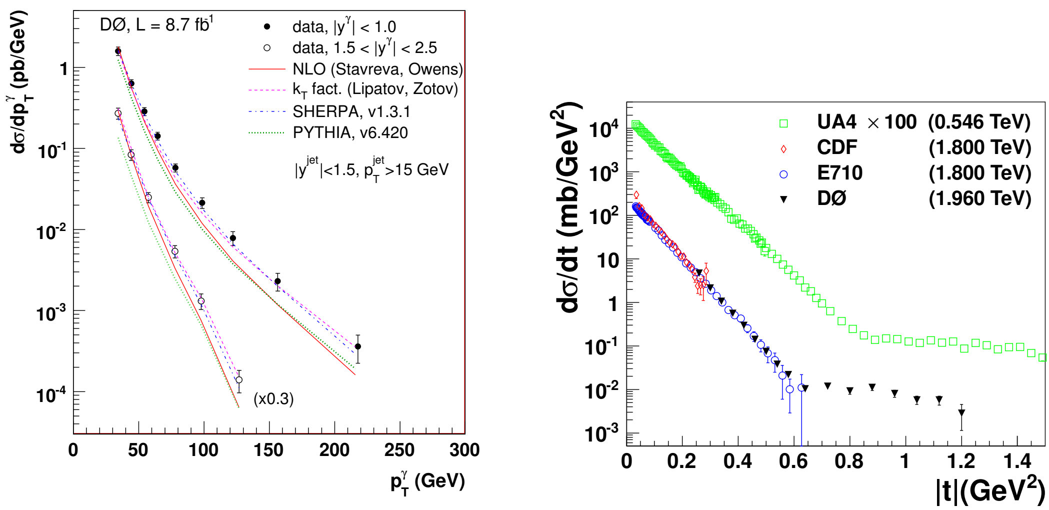

Figure 8. MC closure test of the method used to extract the inclusive jet p_T cross section for the jet $|y| < 0.4$ bin. The full analysis was repeated treating MC events as data and comparing the result to the input cross section. Good agreement is found within the statistical uncertainties of fits to jet energy scale and resolution, and unfolding present in MC (shaded band), which are much smaller than the systematic uncertainties in data (left). $d\sigma/dt$ differential cross section of elastic scattering measured by the D0 Collaboration and compared to the CDF and E710 measurements at $\sqrt{s} = 1.8$ TeV, and to the UA4 measurement at $\sqrt{s} = 0.546$ TeV (scaled by a factor of 100) (right).

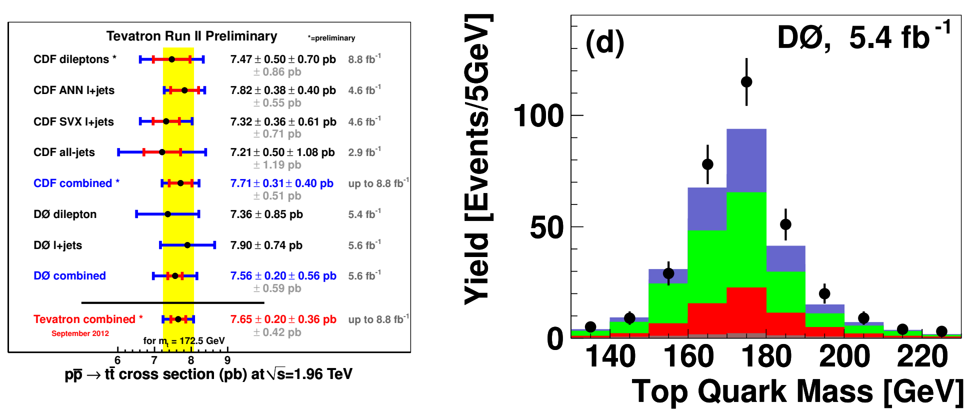

Figure 9. The measurements of $\sigma(t\bar{t})$ cross section from the CDF and D0 experiments (left). Reconstructed mass of top quark from events with 2 leptons and 2 jets (right).

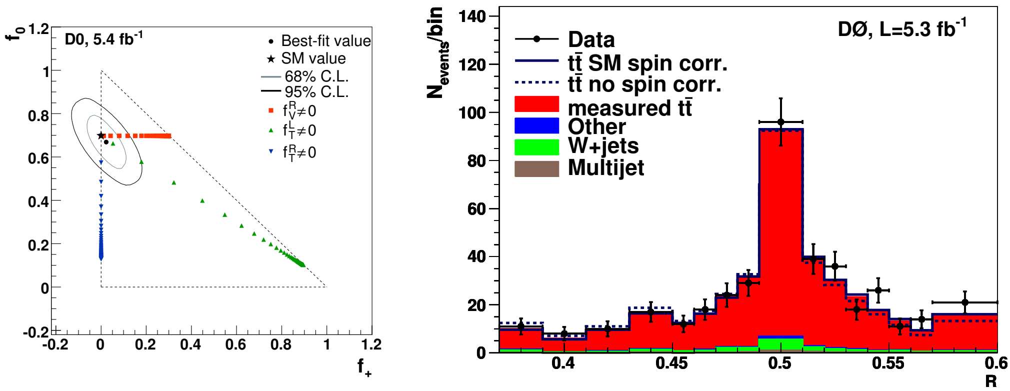

Figure 10. Likelihood contours at the 68% C.L. and the 95% C.L. as a function of W boson helicity fractions. Statistical uncertainties and systematic uncertainties that are uncorrelated with the single top quark measurement are included. The squares, triangles and upside-down triangles show f_V^R , f_T^L and f_T^R varying in fifty equal-size steps such that their ratio to f_V^L goes from zero to ten-to-one. The dashed triangle denotes the physically allowed region. (left). Discriminant R for measurement of top-antitop spin correlation [17](right).

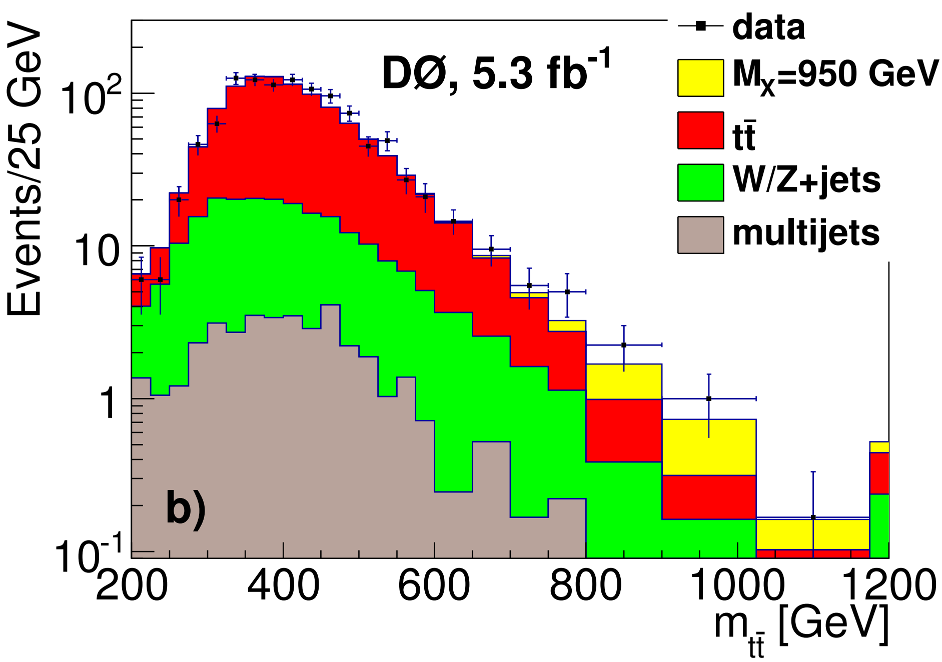

Figure 11. Search for $T\bar{T}$ resonance in mass distribution.

between correlated and uncorrelated top quark spin hypotheses, we define a discriminant R, which is displayed in Fig. 10 together with MC events with and without spin correlation as well as background. Data support the hypothesis with top-antitop spin correlation $C = 0.85 \pm 0.29$ [17] which is in good agreement with the SM prediction.

The total width of top quark Γ_t is extracted from the partial decay width $\Gamma(t \to Wb)$ and the branching fraction $\mathcal{B}(t \to Wb)$. $\Gamma(t \to Wb)$ is obtained from the t-channel single top quark production cross section and $\mathcal{B}(t \to Wb)$ is measured in $t\bar{t}$ events. For a top mass of 172.5 GeV, the resulting width is $\Gamma_t = 2.00^{+0.47}_{-0.43}$ GeV. This translates to a top-quark lifetime of $\tau_t = (3.29^{+0.90}_{-0.63}) \times 10^{-25}$ s [18].

We have also extract an improved direct limit on the CKM matrix element $0.81 < |V_{tb}| \leq 1$ at 95% C.L. and a limit of $|V_{tb}| < 0.59$ for a high mass fourth generation bottom quark assuming unitarity of the fourth generation quark mixing matrix. We searched for a narrow $t\bar{t}$ resonance that decays into a lepton+jets final state based on an integrated luminosity of $5.3 fb^{-1}$ of proton-antiproton collision. We set upper limits on the production cross section of such a resonance multiplied by its branching fraction to $t\bar{t}$ which we compare to predictions for a leptophobic topcolor Z' boson. We exclude such a resonance at the 95% confidence level for masses below $835 GeV$ Fig. 11 [19]. We present new direct constraints on a general Wtb interaction using data corresponding to an integrated luminosity of $5.4 fb^{-1}$. The standard model provides a purely left-handed vector coupling at the Wtb vertex, while the most general, lowest dimension Lagrangian allows right-handed vector and left- or right-handed tensor couplings as well.

We obtain precise limits on these anomalous couplings by comparing the data to the expectations from different assumptions on the Wtb coupling [20].

We present measurements of production cross sections of single top quarks in $p\bar{p}$ collisions at $\sqrt(s) = 1.96 TeV$ [21] in a data sample corresponding to an integrated luminosity of 5.4 fb^{-1}. We select events with an isolated electron or muon, an imbalance in transverse energy, and two, three, or four jets, with one or two of them containing a bottom hadron. We obtain an inclusive cross section of $(p\bar{p} \to tb + X)$,

$\sigma(tqb + X) = 3.43 \pm^{0.73}_{0.74}$ pb and use it to extract the CKM matrix element $0.79 < |V_{tb}| \leq 1$ at the 95% C.L. We also measure $\sigma(p\bar{p}tb + X) = 0.68 \pm^{0.38}_{0.35}$; pb and $\sigma(p\bar{p}tqb + X) = 2.86 \pm^{0.69}_{0.63}$; pb

6 HIGGS boson

We combine searches by the CDF and D0 Collaborations for the associated production of a Higgs boson with a W or Z boson and subsequent decay of the Higgs boson to a bottom-antibottom quark pair.

The data correspond to integrated luminosities of up to $9.7 fb^{-1}$ Fig. 12 [22]. The searches are conducted for a Higgs boson with mass in the range 100 - 150 GeV. We observe an excess of events in the data compared with the background predictions, which is most significant in the mass range between $120 and 135 GeV/c^2$. The largest local significance is 3.3 standard deviations, corresponding to a global significance of 3.1 standard deviations. We interpret this as evidence for the presence of a new particle consistent with the standard model Higgs boson, which is produced in association with a weak vector boson and decays to a bottom-antibottom quark pair [23].

7 New Phenomena

We present the first search for supersymmetry (SUSY) in $Z\gamma$ final states with large missing transverse energy using data corresponding to an integrated luminosity of $6.2 fb^{-1}$ [24]. This signature is predicted in gauge-mediated SUSY-breaking models, where the lightest neutralino is the next-to-lightest

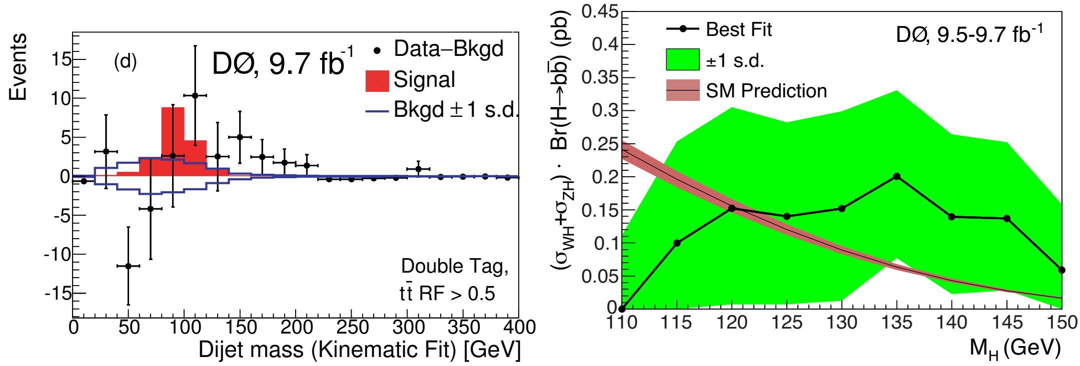

Figure 12. Background-subtracted distribution of the reconstructed dijet mass m_{jj} , summed over all input channels. The *VZ* signal and the background contributions are fit to the data, and the fitted background is subtracted. The fitted VZ and expected SM Higgs, $m_H = 125GeV$ contributions are shown with filled histograms (left). The dark and light-shaded regions indicate the 1 s.d. and 2 s.d. measurement uncertainties, and the SM prediction is shown as the smooth, falling curve with a narrow band indicating the theoretical uncertainty. The expected cross section fit values assuming the SM Higgs boson is present at $m_H = 125GeV/c^2$ SM rate (dark blue) and the best fitted rate from data (light magenta) (right).

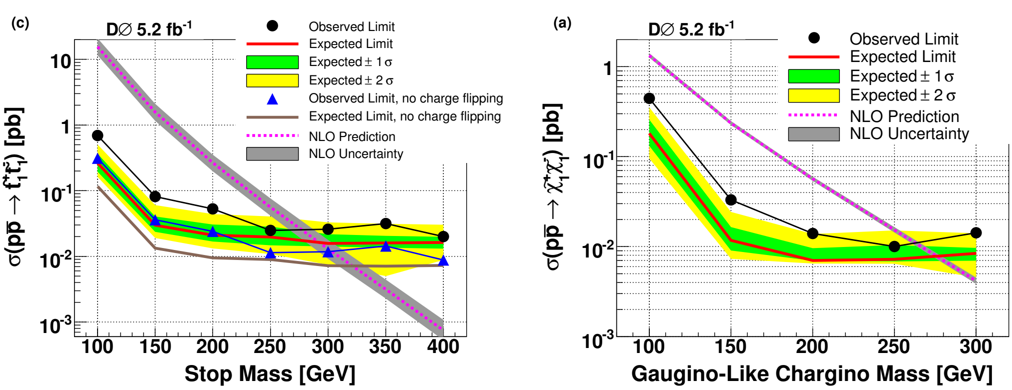

Figure 13. Search for Stop quark and Gauging-like Chargino masses (left).

supersymmetric particle (NLSP) and is produced in pairs, possibly through decay from heavier supersymmetric particles. The NLSP can decay either to a Z boson or a photon and an associated gravitino that escapes detection. We exclude this model at the 95% C.L. for SUSY breaking scales of $\Lambda < 87TeV$, corresponding to neutralino masses of $< 151GeV$.

We present a search for Kaluza-Klein (KK) particles predicted by models with universal extra dimensions (UED) using a data set corresponding to an integrated luminosity of 7.3 fb^{-1} [25]. The decay chain of KK particles can lead to a final state with two muons of the same charge. This signature is used to set a lower limit on the compactification scale of $R^{-1} > 260$ GeV in a minimal UED model.

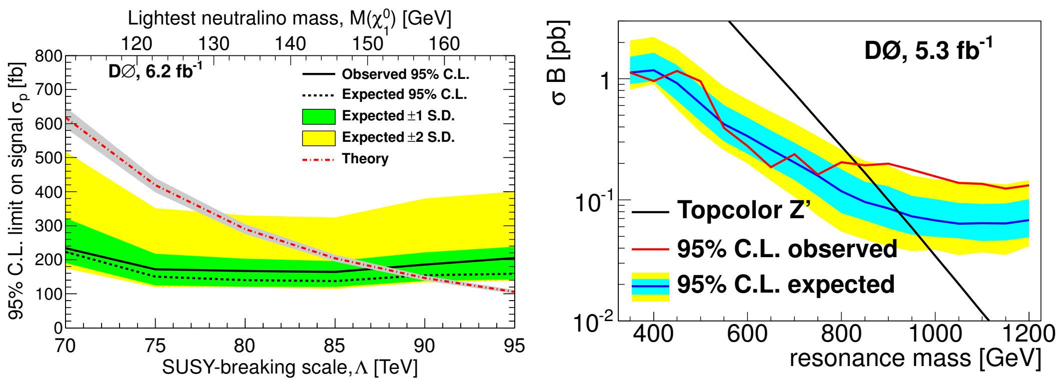

Figure 14. Search for Neutralino and new Z boson decaying into top-antitop pair.

The Tevatron has finished data taking, but the analysis of data with full statistics of reconstructed events will still continue and new results will comme in the next year.

References

[1] Measurement of the Semileptonic Charge Asymmetry using B0 meson mixing with the D0 detector, Phys. Rev. D, arXiv:1208.5813.

[2] Measurement of the Relative Branching Ratio of $B_s^0 J/\psi f_{(}^{0}980)/f_{980}^{0}$ to $B_s^0 J/\psi$ Phys. Rev. D 85, 011103 (2012).

[3] Measurement of the Λ_b^0 Lifetime in the Exclusive Decay $\Lambda_b^9 \to J\psi\Lambda^0$ Phys. Rev. D 85, 112003 (2012).

[4] Measurement of the B^0 Lifetime in the Exclusive Decay B^0 J/ψ K_s^0, Phys. Rev. D 85, 112003 (2012).

[5] Observation of a Narrow State Decaying into $\upsilon(1S) + \gamma$, Phys. Rev. D 86, 031103(R) (2012).

[6] Combination of CDF and D0 Measurements of the W Boson mass, Phys. Lett. B 714, 32 (2012).

[7] Measurement of the W Boson Mass with the D0 Detector, Phys. Rev. Lett. 108, 151804 (2012).

[8] Measurement of the WZ and ZZ Production Cross Sections using Leptonic Final States, Phys. Rev. D 85, 112005 (2012).

[9] Measurements of WW and WZ Production in $W + jets$, Phys. Rev. Lett. 108, 181803 (2012).

[10] Measurement of the Inclusive Jet Cross Section in pp Collisions, Phys. Rev. D 85, 052006 (2012).

[11] Measurement of the Photon + b-Jet Production Differential Cross Section in pp Collisions, Phys. Lett. B 714, 32 (2012).

[12] Measurement of the Differential Cross Section $d\sigma/dt$ in Elastic $p\bar{p}$ Scattering at $\sqrt{s} = 1.96 TeV$, Phys. Rev. D 86, 012009 (2012).

[13] Measurement of the Top Quark Mass in pp Collisions using Events with Two Leptons,Phys. Rev. D 86 051103(R) (2012).

[14] Measurement of Leptonic Asymmetries and Top Quark Polarization in tt Production, Phys. Rev. Lett.

[15] Combination of Searches for Anomalous Top Quark Couplings, Phys. Lett. B 713, 165 (2012).

[16] Combination of CDF and D? Measurements of the W Boson Helicity in Top Quark Decays Phys. Rev. D 85, 071106 (2012).

[17] Evidence for Spin Correlation in $t\bar{t}$ Production, Phys. Rev. Lett. 108, 032004 (2012).

[18] Improved Determination of the Width of the Top Quark, Phys. Rev. D 85, 091104 (2012).

[19] Search for a Narrow $T\bar{T}$ Resonance in pp Collisions at $\sqrt(s) = 1.9TeV$, Phys. Rev. D 85, 051101 (2012).

[20] Search for Anomalous Wtb Couplings in Single Top Quark Production, Phys. Lett. B 708, 21 (2012).

[21] Measurement of the Top Quark σ Phys. Rev. D 86 051103(R) (2012).

[22] Search for the standard model Higgs boson in associated WH production in $9.7fb^{-1}$ of $p\bar{p}$ collisions with the D0 detector, Phys. Rev. Lett. 109, 121804 (2012).

[23] Combined search for the standard model Higgs boson decaying to $b\bar{b}$, Phys. Rev. Lett. 109, 121802 (2012).

[24] Search for $Z\gamma$ Events with Large Missing Transverse Energy, Phys. Rev. D 86, 071701(R) (2012).

[25] Search for Universal Extra Dimensions in pp Collisions, Phys. Rev. Lett. 108, 131802 (2012).

[26] Gaugino Search for Charged Massive Long-Lived Particles, Phys. Rev. Lett. 108, 121802 (2012).